DOI: https://doi.org/10.24425/amm.2024.149792

S. MISTREANU[1], F. TUDOSE-SANDU-VILLE[2*], C. MUNTEANU[2], R. CIMPOESU[1*], M. LUTCANU[1,3], I. ȘTIRBU[1], V. MANOLE[1], C. STAMATE, O. RUSU[1], N. CIMPOEȘU[1]

INFLUENCE OF CORROSION ON THERMO-MECHANICAL CONTACT FATIGUE IN ROLLING CONDITIONS WITH LOW AMPLITUDE SLIDING

The paper presents some aspects concerning mechanical contact fatigue and corrosion wear and the links of these two kinds of wear in the common deterioration of the contact layer. The surface state, for both presented areas, is analyzed using scanning electron microscopy (SEM) and energy dispersive spectroscopy (EDS) in order to confirm the double action of corrosion and wear during the experimental test. 2 and 3D insights were taken from the worn area, corrosion compounds were identified and analyzed. Linear and cyclic potentiometry were performed on the base materials after the OCP was established in salt solution. When the level of the thermal and the mechanical stress are located at the same depth under the contact surface the resulting stress is greater and has the opportunity to develop the first crack to the surface. The metallic material surface presents a double type of corrosion: one based on oxidation and the other one based on oxidation plus wear (tribo-corrosion), the difference is being given by the material quantity and type involved.

Keywords: Thermo-mechanical contact fatigue; corrosion wear; Jacq thermal anomaly

1. Introduction

The fatigue behavior of metallic materials in general and of steels in particular has been analyzed in recent decades, and it remains a relevant problem for many applications on an industrial scale. In many cases, based on the demands to which the active elements are subjected, contact fatigue has recently become significant. The analysis of total fatigue failure of metallic materials under contact stresses is an important scientific and practical problem. Often the cyclic resistance of various materials under fatigue contact loading is evaluated according to the lamination scheme [1]. However, in this case, crack initiation occurs mostly in the underground layers [2-4]. Meanwhile, under contact loading according to the pulsating loading scheme, the crack initiation mainly starts from the surface [5]. In engineering applications, friction is a phenomenon that causes wear, i.e. material removal. Along with other effects like e.g. severe plastic deformation and adhesion, strongly affects the surface and near-surface morphology of the material, i.e. topography, grain size, dislocation density and the formation of new phases [6]. The microstructure of steels can be either stable or metastable against strain-induced phase transformations and is decisive for material behavior [7,8]. It is therefore instructive to compare the microstructural changes caused by sliding in these two qualitatively different groups of materials [9-11]. The laboratory results, nowhere in the literature, were not compared directly with the industrial results because of the lack of a proper equipment. In our case we use an industrial equipment in laboratory tests.

This article presents the results obtained from the analysis of the corrosion resistance of the OLC45 material requested on a laboratory equipment made by the authors and on a potentiostat equipment using a three-electrode work cell. The results were compared with the corrosion of a OLC45 roll from a hot rolling equipment used for steel rolling in order to determine the influence of corrosion process on the general degradation of a rolling equipment roll during operation.

2. Experimental details

The material used for experiments is a non-alloyed steel named C45 with industrial applications in many manufactured states including laminated. Chemical composition of the material (mass percentages) is given in TABLE 1. The material in initial

1 GHEORGHE ASACHI UNIVERSITY OF IASI, FACULTY OF MATERIALS SCIENCE AND ENGINEERING, 43 DIMITRIE MANGERON STR., 700050, IASI
2 GHEORGHE ASACHI UNIVERSITY OF IASI, FACULTY OF MECHANICS, MECHANICAL ENGIN EERING, MECHATRONICS AND ROBOTICS, 43 DIMITRIE MANGERON STR., 700050, IASI
3 GHEORGHE ASACHI UNIVERSITY OF IASI, DEPARTMENT OF PHYSICS, 67 DIMITRIE MANGERON STR., 700050, IASI
* Corresponding author: ramona.cimpoesu@tuiasi.ro

state present a reduced hardenability in both cooling medium water or oil however the heat treatment is proper for surface hardening providing this material a bigger hardness. By weld ability point of view based on the medium-high C percentage the procedure can be applied with few precautions.

TABLE 1

Chemical composition %wt of steel OLC45 (1.0503): EN 10277-2-2008 [12]

Cr + Mo + Ni = max 0.63 [wt%]							
C	**Si**	**Mn**	**Ni**	**P**	**S**	**Cr**	**Mo**
0.43-0.5	max. 0.4	0.5-0.8	max. 0.4	max. 0.045	max. 0.045	max. 0.4	max. 0.1

The main wear test conditions are as follow: The direct solicitation on the surface of 6÷25 KN (normal force), and developing a normal contact stress of σ_{max} = 185÷400 MPa, the contact stain width between 10÷20 mm, roller characteristics: B_{roller} width = 30÷50 mm, $D_{ext\ max}$ (diameter): 116 mm, B_{roller} width contact between 5÷15 mm and D_{ext} min diameter of 111 mm, D_{int} diameter between 50÷80 mm; Rotation rate n = 125 rev/min, same for all rollers in contact. Roller Material: OLC45 x B/3 STAS 880-88 Characteristics: Φ 120, norm of dimensions 333-87, length 4 m/PCs and chemical composition: C = 0,47%, Mn = 0,63%, Si = 0.26%, Cr = 0.22%, Ni = 0.14%, Cu = 0.14%, Al = 0,032%, corresponding to the discharge test [2].

Mechanical properties are: $R_{p0.2}$ = 688 N/mm^2; R_m = 796 N/mm^2; A = 21% ; Z = 65%. In Fig. 1 pictures with the test rings from diverse positions are presented: a) top view, b) detail of the top view, c) contact areas and d) experimental heated cylinders.

During the first test period (1-3 h) the rolling contact is with no cooling heating to bring the rolls to a significant temperature for the test. Then the heating and cooling are applied to different surfaces at the same time to make the difference of temperature ΔT in the roller wall. The test for the three rolls set (two "cold" and the "hot" rolls) will be fulfilled when the first signs of deterioration in the contact surfaces appear after 24-36 h, [5].

The cooling water affects corrosion wear on the outer surface of the cool rolls. The first signs of deterioration showed as some cracks developed under the corrosion layer determined by the cooling water. In the rolling process with very small sliding, this corrosion layer is removed by the small sliding movement determined by the difference of the contact diameter of the rolls. It is observed some freight corrosion aspects on the contact surface.

The surface state was analyzed using scanning electron microscopy (SEM: VegaTescan LMH II, SE detector, 30 kV) and energy dispersive spectroscopy (EDS: Bruker) after the thermo-mechanical tests. Images of the surface in 2D and 3D were realized in order to compare the state of the sample in corroded and worn areas, respectively. As an experimental sample, a C45 piece of the roll was used for the electro-corrosion resistance tests. The behavior at electro-corrosion of the experimental material was analyzed using the potentiostat PGZ301 equipment using a three electrodes cell. The electrolyte solution was industrial normal water. Surfaces of the metallic material were compared after both types of corrosion [13,14].

a) b)

a) b)

Fig. 1. Images with the test rig from diverse positions a) top view, b) detail of the top view, c) contact areas and d) experimental heated cylinders

3. Experimental results

The surface of the active heated role was analyzed through scanning electron microscopy (2D and 3D insights). Also, consideration of the chemical composition of the surface (for both worn and corroded areas) was taken using energy dispersive spectroscopy. At the same time, the authors performed a test of resistance for the electro-corrosion test in order to evaluate the behavior of the experimental material OLC45 (1.0503) based on standard EN 10277-2: 2008 [12].

3.1. Structure and chemical analysis of the contact surface affected by corrosion

Surface analysis was made doing some preliminary tests on the experimental sample surface. The main results are given in Fig. 2 by scanning electron microscopy (SEM). SEM images for the roll surface a) interface image between the worn and corroded area of the material, b) corroded area, c) and d) worn area at 100× respectively 500×, e) 3D image of the surface and d) optical sample profile. The surface presents two separate areas

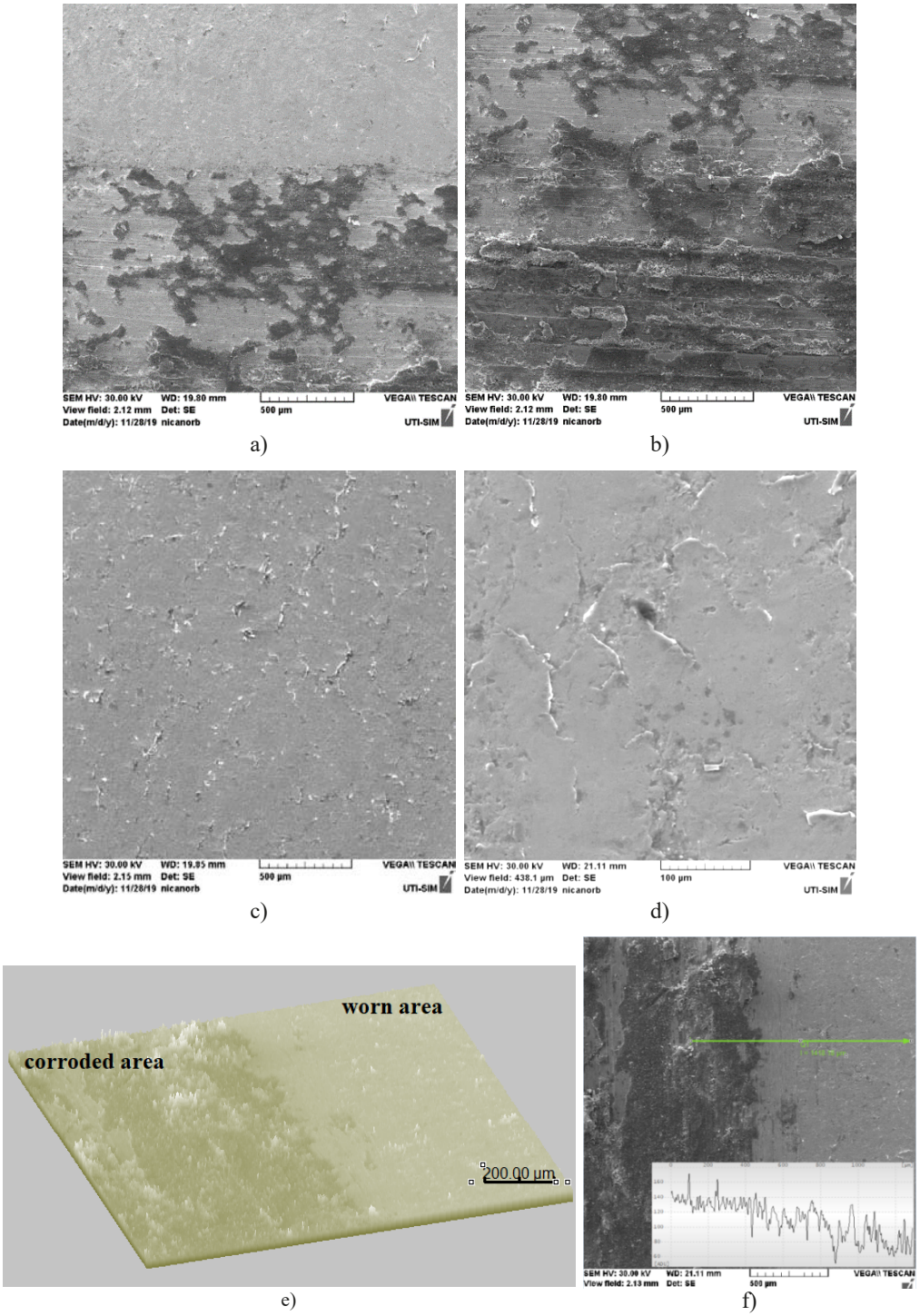

Fig. 2. SEM images of the roll surface a) interface image between the worn and corroded area of the material, b) corroded area, c) and d) worn area at 100× respectively 500×, e) 3D image of the surface and d) optical sample profile

– Fig. 2a)-d), one is connected to de worn surface, the other on the corroded (water influenced) area.

Both 2 and 3 D areas present similar results, Fig. 2, about the surface state of the material. In the worn surface, Fig. 2a) – half c) and d), the deformed by wear process stains are presented. The eroded surface, by wear, Fig. 2e) and f) is evidenced by the 3D image and profilometry of the decreased surface.

Fig. 3 is presented the chemical composition analysis using qualitative analysis in a) through energy identification and in b) semi-quantitative determination. Normal weight and atom quantifications are done. Beside the main elements of the metallic material can be observed an oxidation state of the material and potassium presence from the cooling liquid of the experimental system.

In Fig. 4 the elemental distribution on the selected area a), and each element separately b)-i) are presented. On the corroded area, the bottom side of the selected image, Fig. 4a), a higher presence of oxygen and carbon elements is observed, Figs. 4b) and 4c) but on the worn surface, top side, the metallic and non-metallic compounds are mechanically removed by the wear process.

In Fig. 5 the differences between the corroded area and the worn surface is presented through the line variations of main chemical elements identified on the entire metallic surface. The lack of iron signal on the corroded area is based on the thickness of the oxides and carbonates compounds formed on top of the Fe-based material that cover the surface. Based on the wear direction we also can observe small oxide areas left on the surface.

3.2. Electro-corrosion resistance of the experimental samples in laboratory conditions

Cyclic voltammetry consists in reducing the electrical potential of the electrode in the positive direction, up to a determined value of current or potential. After scanning, care it is immediately possible to stretch more negatively until the potential reached. It should be emphasized that although the electrochemical method is the fastest method of determining the corrosion rate, in some cases it may be susceptible to large errors or dubious results. For this reason, the evaluation of the corrosion rate based on the polarization resistance method should be compared, as far as possible, with the gravimetric method [15-17]. More complete information can be obtained by chemical analysis of the corrosion medium after the polarization process and/or by determining the weight loss of the sample. This analysis, carried out with very sensitive methods, can provide information on the ionic species passed from the metal into the solution as well as on the chemical transformations of the species in the solution [18,19].

The re-passivation potential is located in the range of negative values (–50 mV vs. ESC), the potential that can occur in the form of currency in the oral cavity. The curve $j = f(E)$, Fig. 6b) shows an advanced corrosion resistance up to an over potential of over 500 mV (ESC). Above this potential, a uniform (generalized) corrosion process begins to manifest itself, reflected by increasing current density. The cyclical polarization curves have a generalized corrosion aspect an experimental of the surface alloys.

If they can be repeated for a determination of some product changes about the current scan potential storage curve. If the cyclical polarization curve (cyclic voltammogram) is encountered, there can no longer be historical; the cathodic branch of the voltammogram is practically superimposed on the anodic branch, with the exception of a narrow potential area located in the vicinity of the non-dissolving care potential [20,16]. So far, a cathode can be unloaded from the branch, which can be explained by changes in the surface of the sample as a result of corrosion (as a result of corrosion remaining metal when the current cadence of the drop can be made). The very small

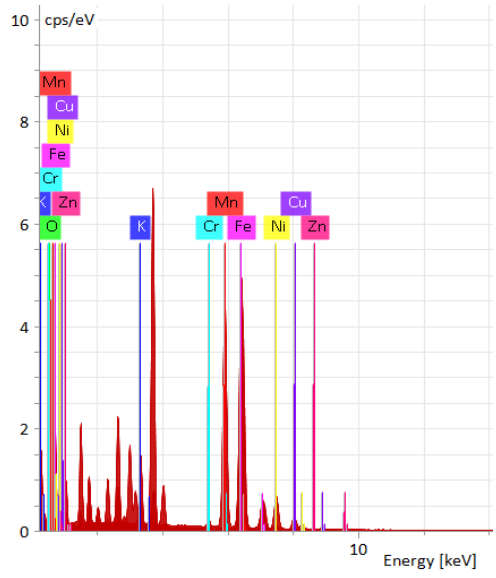

a)

Element	Mass Norm. [%]	Atom [%]	abs. error [%] (1 sigma)
Iron	83.74	64.05	2.2
Oxygen	12.33	32.91	2.01
Manganese	2.17	1.68	0.1
Potassium	0.30	0.33	0.05
Zinc	0.46	0.30	0.07
Nickel	0.38	0.27	0.07
Copper	0.38	0.26	0.07
Chromium	0.24	0.2	0.05
	100	100	

b)

Fig. 3. Chemical composition analysis a) energy identification and b) quantitative determination

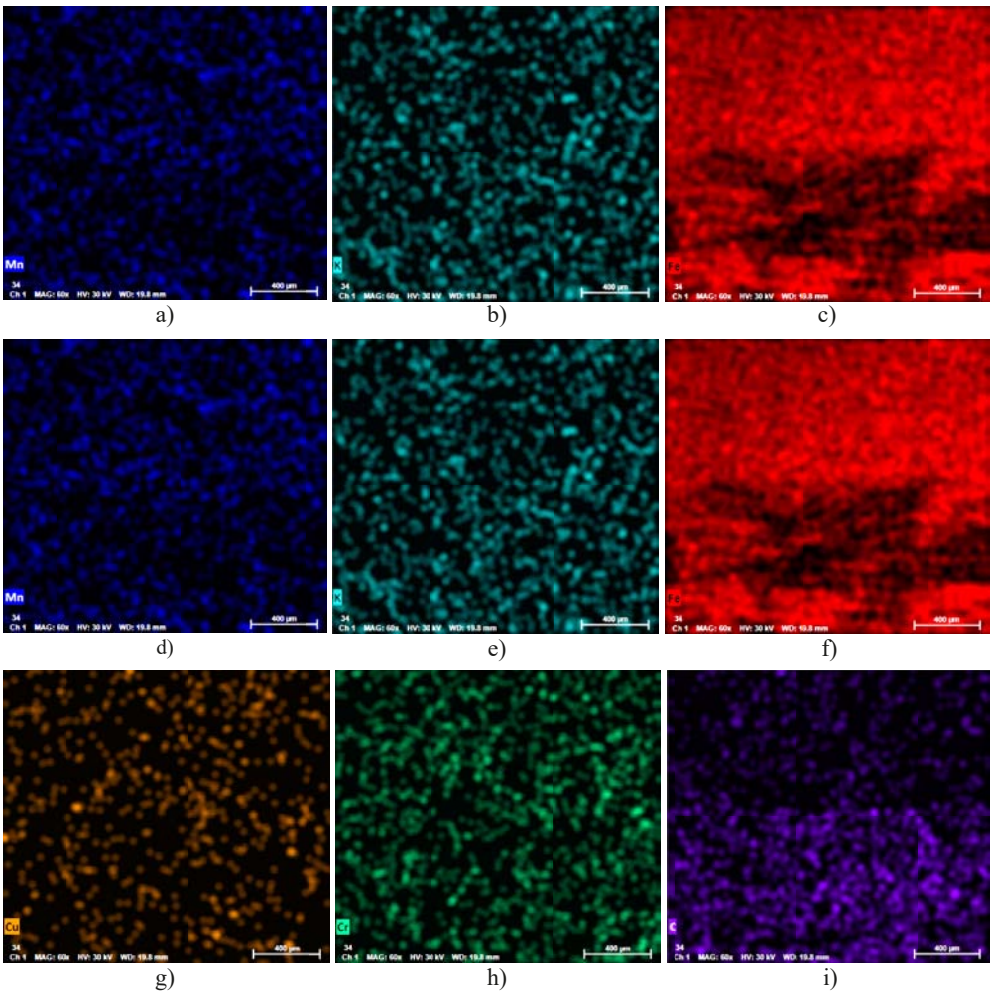

Fig. 4. Elemental distribution on the selected area a), and each element separately b) O, c) Ni, d) Mn, e) K, f) Fe, g) Cu, h) Cr and i) C.

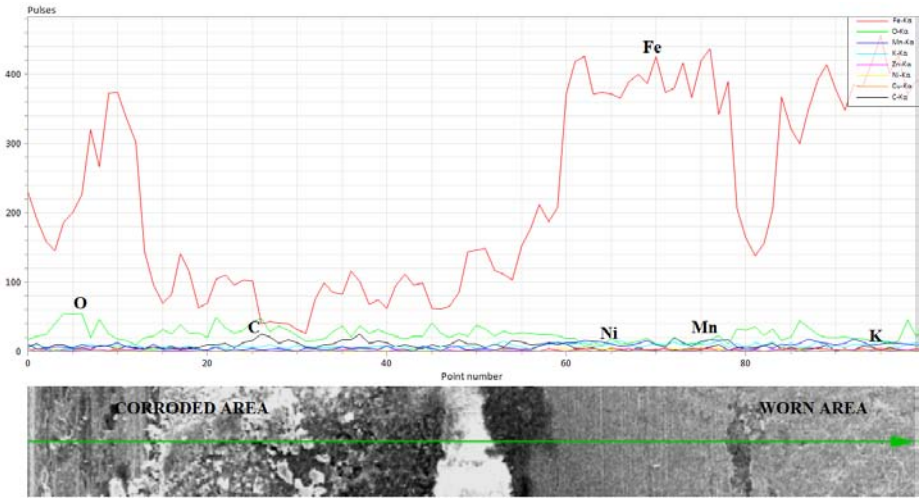

Fig. 5. Line variations of main chemical elements identified on the surface

TABLE 2

Electro-chemical resistance of the experimental alloy in water

Parameters/ experimental rate	***E*(*i* = 0) mV**	**Beta *a* mV**	**Beta *c* mV**	**$i_{corrosion}$ mA/cm^2**	***Rp* ohm.cm^2**	**r_{cor} mm/Year**
Rate 1 (1 mV/sec)	–733.6	147	–161.1	0.1144	182.52	0.70
Rate 2 (5 mV/sec)	–587.8	124.0	–440.2	0.2758	117.74	1.69
Rate 3 (10 mV/sec)	–738.0	130.7	200.8	0.2679	76.38	1.64

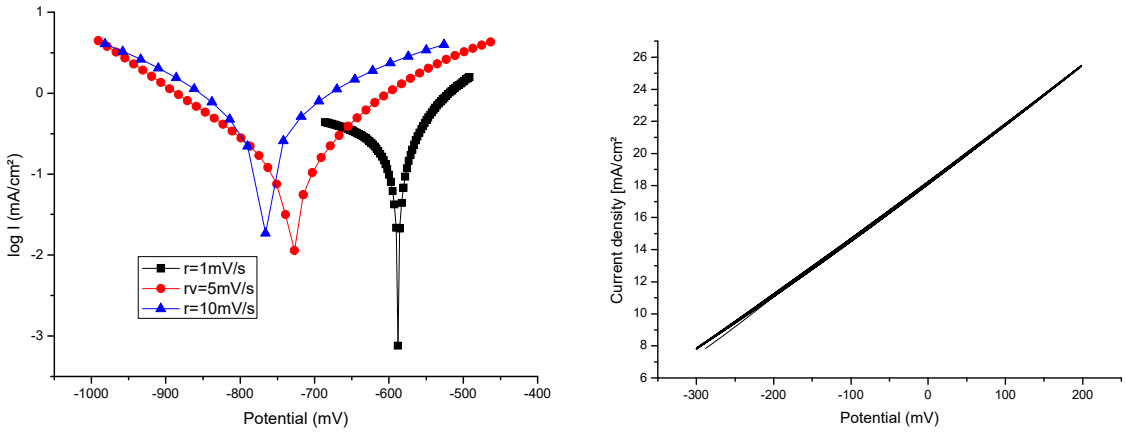

a) b)

Fig. 6. Electro-corrosion test a) linear potentiometry and b) cyclic potentiometry

area is a loop of cyclic curves reflecting or creating an area of general corrosion (less pitting points) [21,22]. On the other hand, the potential for re-passivation is very small, closer to the potential for corrosion it has been possible to extend, the imperfect passivation range, (Es–Erp), is very high, so this care may be considered inadequate. The part from you see the corrosion resistance [23,24].

In Fig. 7 are presented SEM images of the corroded surface at different amplification powers type: a) 200×, b) 500× and c) 2000×.

The surface presents obviously a general corrosion characteristic for normal steels used in applications. In Fig. 8 the spectral identification of the chemical elements on a corroded selected area of the experimental steel is presented.

In TABLE 3, quantification of chemical composition determined on the surface is given in weight and atomic percentages.

The carbon quantification in EDS detectors is known as an analysis which presents high errors but the surface presents also a high degree of oxidation based on the corrosion process. In Fig. 9 the elemental distributions on a selected area of Fe, O, Mn ,C are presented.

General corrosion behavior is observed on the entire surface with the presence of the oxides attached to some parts.

TABLE 3

Chemical composition of the surface

Element	Mass Norm. [%]	Atom Norm [%]	abs. error [%] (1 sigma)
Iron	71.41	40.47	1.9
Carbon	13.69	36.10	3.1
Oxygen	10.59	20.94	1.8
Manganese	4.31	2.48	0.2
	100	100	

No evidence of special elemental removal is observed and also no compounds like salts or chlorides were identified on the surface.

4. Conclusions

From experimental results few conclusions can be drawn:

– thermo-mechanical contact fatigue made a generalized corrosion and cracking of the surface (he surfaces with developed cracks determined an important level of noise and vibration in exploitation of the equipment).

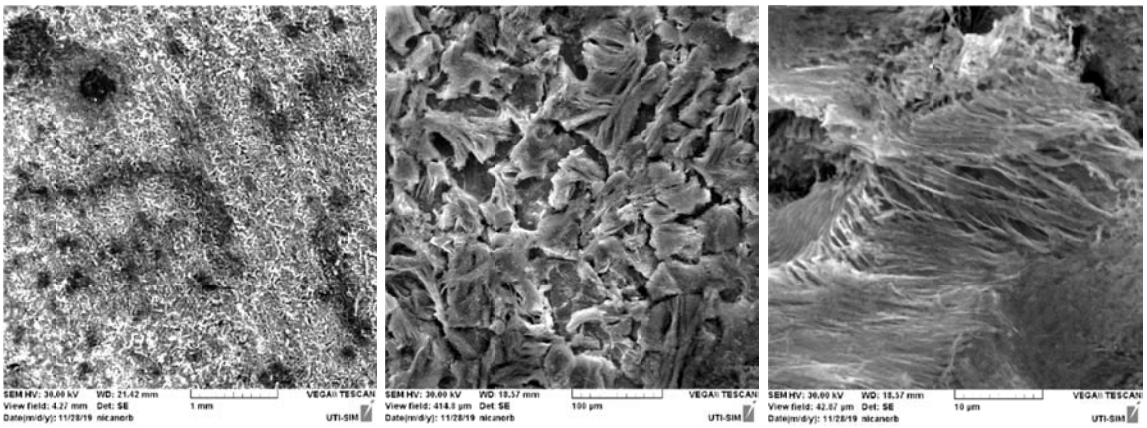

a) b) c)

Fig. 7. SEM images of the corroded surface a) 200×, b) 500× and c) 2000×

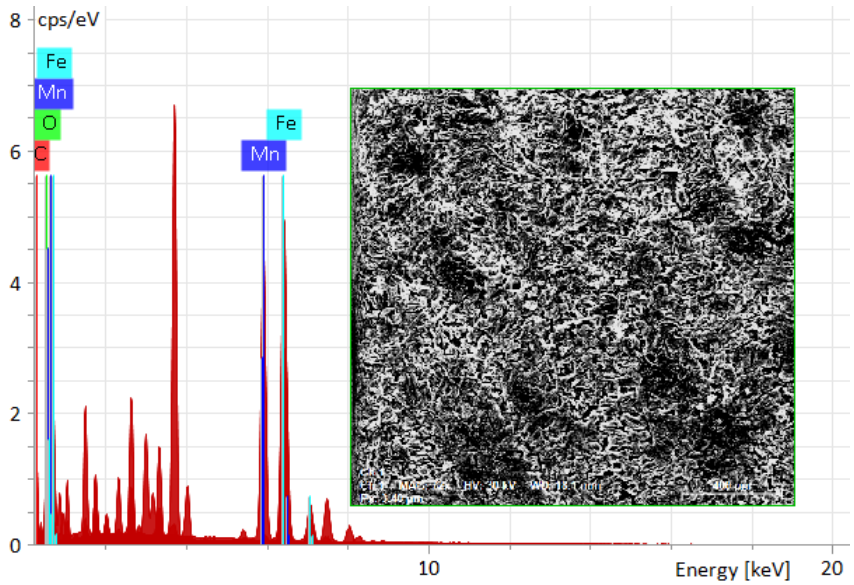

Fig. 8. Spectral identification of the chemical elements on a corroded selected area

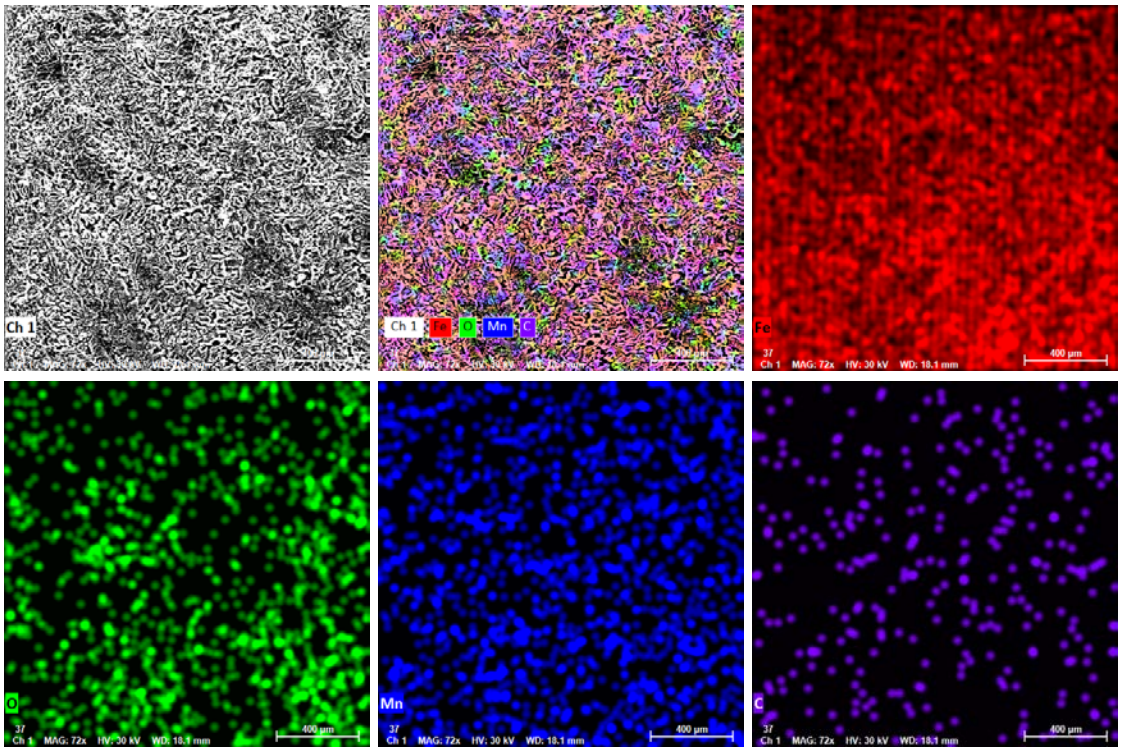

Fig. 9. Elemental distributions on a selected area of Fe, O, Mn and C

– Corrosion wear presenting as rust or freight corrosion influence the installation of thermo-mechanical contact fatigue by accelerating the first appearance of deterioration.
– When the level of the thermal and the mechanical stress are located at the same depth under the contact surface the resulting stress is greater and has the opportunity to develop the first crack to the surface (such conditions determine the presence of thermo-mechanical contact fatigue deterioration on the contact surface).
– The metallic material surface presents a double type of corrosion: one based on oxidation and the other one based on oxidation plus wear (tribo-corrosion), the difference being given by the material quantity and type involved, both presented using an EDS detector.

Acknowledgements

This research was funded by by Ministry of Research, Innovation and Digitization, project FAIR_09/24.11.2020, the Executive Agency for Higher Education, Research, Development and Innovation, UEFISCDI, ROBIM-project number PN-III-P4-ID-PCE2020-0332.

REFERENCES

[1] F. Tudose-Sandu-Ville, Appl. Mech. Mater. **658**, 377-380 (2014).

[2] F. Tudose-Sandu-Ville, IOP Conference Series Materials Science and Engineering **147** (1), 012007 (2016).

[3] V. Paleu, C.C. Paleu, B. Istrate, S Bhaumik, C. Munteanu, IOP Conference Series-Materials Science and Engineering **724**, 012064 (2020).

[4] V.V. Savinkin, Z.Z. Zhumekenova, A.V. Sandu, P. Vizureanu, S.V. Savinkin, S.N. Kolisnichenko, O.V. Ivanova, Coatings **11**, (12)1441 (2021).

[5] G.B. Sinclair, J.E. Helms, A review of simple formulae for elastic hoop stresses in cylindrical and spherical pressure vessels: What can be used when, / International Journal of Pressure Vessels and Piping **128**, 1-7 (2015).

[6] M. Panturu, D.L. Chicet, C. Munteanu, B Istrate, P. Avram, IOP Conference Series-Materials Science and Engineering **444,** 032009 (2018).

[7] G.L. Pintilei, V.I. Crismaru, M. Abrudeanu, C. Munteanu, D. Luca, B. Istrate, Appl. Surf. Sci. **352**, 169-177 (2015).

[8] P. Avram, M.S. Imbrea, B. Istrate, S.I. Strugaru, M. Benchea, C. Munteanu, Indian J. Eng. Mater. S. **21** (3), 315-321 (2014).

[9] E. Bettini, C. Leygraf, C. Lin, P. Liu, J. Pan, J. Electrochem. Soc. **159**, C422-C427 (2012).

[10] A.O.F. Hayama, P.N. Andrade, A. Cremasco, R.J. Contieri, C.R.M. Afonso, R. Caram, Mater. Des. **55**, 1006-1013 (2014).

[11] C. Liu, E. Zhang, J. Mater. Sci. Mater. Med. **26**, 142 (2015).

[12] EN 10277-2: 2008

[13] D. Mareci, N. Cimpoesu, M.I. Popa, Materials and Corrosion, 63-11, 176-180 (2012).

[14] M. Zaharia, S. Stanciu, R. Cimpoeșu, I. Ioniță, N. Cimpoeșu, Appl. Surf. Sci. **438**, 20-32 (2018).

[15] N. Cimpoeşu, F. Săndulache, B. Istrate, R. Cimpoeşu, G. Zegan, Metals **8** (7), 541 (2018).

[16] J. Izquierdo, G. Bolat, N. Cimpoesu, L C. Trinca, D. Mareci, R.M. Souto, Appl. Surf. Sci. **385**, 368-378 (2016).

[17] N. Cimpoeșu, L.C. Trincă, G. Dascălu, S. Stanciu, S.O. Gurlui, D. Mareci, Journal of Chemistry. Article ID 9520972 (2016)

[18] A.V. Sandu, Materials **14** (21), 6606 (2021).

[19] K. Yamanaka, M. Mori, A. Chiba, Mater. Lett. **116**, 82-85 (2014).

[20] S.L.d. Assis, I. Costa, Mater. Corros. **58**, 329-333 (2007).

[21] F. Rosalbino, G. Scavino, Electrochim. Acta **111**, 656-662 (2013).

[22] A.V. Sandu, A. Ciomaga, G. Nemtoi, C. Bejinariu, I. Sandu, Microsc. Res. Techniq. **75**, (12) 1711-1716 (2012).

[23] P. Zieba, M. Chronowski, J. Opara, O.A. Kogtenkova, B.B. Straumal, Discontinuous Dissolution Reaction in a Fe-13.5 at. % Zn Alloy. Materials **14** (8), 1939(2021).

[24] R. Cimpoesu, P. Vizureanu, I. Stirbu; A. Sodor, G. Zegan, M. Prelipceanu, N. Cimpoesu, N. Ioanid, Corrosion-Resistance Analysis of HA Layer Deposited through Electrophoresis on Ti4Al4Zr Metallic Substrate. Applied Sciences **1** (9), 4198 (2021).